

Thermal characterization of micro thermoelectric coolers: an analytical study

This content has been downloaded from IOPscience. Please scroll down to see the full text.

2014 J. Phys.: Conf. Ser. 547 012007

(<http://iopscience.iop.org/1742-6596/547/1/012007>)

View [the table of contents for this issue](#), or go to the [journal homepage](#) for more

Download details:

IP Address: 192.150.195.22

This content was downloaded on 20/11/2014 at 16:49

Please note that [terms and conditions apply](#).

Thermal characterization of micro thermoelectric coolers: an analytical study

G De Aloysio¹ and F de Monte²

¹Department of Information Engineering, Computer Science and Mathematics,
University of L'Aquila, Via Vetoio, 67100 L'Aquila, ITALY

²Department of Industrial and Information Engineering and Economics,
University of L'Aquila, Via Gronchi 18, 67100 L'Aquila, ITALY

E-mail: giulia.dealoytio@graduate.univaq.it

Abstract. Aim of this paper is to provide a complete characterization of the transient thermal behaviour of thermoelectric (TE) micro-coolers by solving the parabolic heat diffusion equation, through two different analytical methods, the Laplace Transform (LT) and the Separation of Variables (SOV). The results of the performed analysis show that a numerical inversion of the Laplace Transform is necessary, because the analytical-based Riemann-sum approximation does not yield temperature values at very early times. Once the temperature distribution is known in both the semiconductors of the p-n junction, the heat fluxes and the coefficient of performance (COP) of the cooler may be obtained. Then, by applying the proposed procedure to an existing micro-TE cooler, it is observed that the cooling load and the COP reach their maximum values, 2.9 W and 2, respectively, at different times, 3.4 ms vs. 1.7 ms. When a steady-state is reached, the micro-system is characterized by a cooling load of about 1.9 W with an efficiency of nearly 0.5, both in agreement with experimental and numerical data.

1. Introduction

Thermoelectric devices are solid state energy converters which can convert electricity into thermal energy for cooling purposes or thermal energy into electricity for power generation.

Based on semiconductor materials, these systems offer many advantages compared with conventional fluid-based devices:

- High reliability due to the absence of moving parts (no extra-maintenance).
- Absence of refrigerants which are harmful for the environment.
- No waste matter in the conversion process.

As the interest in micro- and nanotechnology has increased in the last years, miniature thermoelectric systems attract a lot of attention, in particular the micro-TEC devices because they offer effective cooling in micro-processors and in other microelectronic applications [1,2].

A TEC is composed of pairs of thermoelements, p-type and n-type semiconductors, and copper interconnectors at the top and at the bottom of the semiconductors. These thermoelectric elements are connected electrically in series and thermally in parallel. If an electric current is applied, the charged carriers in the material (electrons and holes) diffuse from the cold side to the hot side, leaving behind their oppositely charged and immobile nuclei [3], so that a temperature difference is produced. This



temperature difference drives the phonons drift back to the cold side, so that heat conduction arises at equilibrium. Many attempts have been made to improve the performances of TEC, such as the design of nanostructured thermoelectric materials, nanocomposites, for instance alloys of Bi_2Te_3 , as they are the best thermoelectric materials at room temperature.

However, it is important to understand the thermal behaviour of these devices in order to improve their performance. Most of the existing models focus on thermal behaviour under steady state conditions, whereas only a few papers [1,3,4,5,7,8] analyse the transient thermal behaviour of micro-thermoelectric devices. The dynamic characteristics play an important role in operation of micro thermoelectric coolers, especially during start-up and shut down and in case of variable operational parameters. In the last years different complete three-dimensional models [3,6-9] have been proposed to investigate the dynamic behaviour of miniature TECs, but despite their completeness, they provide solutions by means of numerical methods.

Starting from the available in the literature models [3-10], the aim of this paper is to provide an analytical study of the transient behaviour of micro- thermoelectric coolers, including the Thomson effect. In order to obtain the temperature distributions for both the semiconductors, the governing equations of the semiconductors (i.e. the parabolic heat diffusion equations with boundary conditions of first kind and initial uniform condition) are solved through the Laplace Transform (LT) and the Separation of Variables (SOV) Methods. The temperature solution is then implemented in MATLAB® ambient. In particular a comparison among the SOV Method, the analytical and a numerical inversion of Laplace Transform is presented. Once the temperature distributions are known, the heat fluxes and the COP of the micro cooler may be obtained. The influence of the Thomson effect on the performance of the micro-TEC is analysed under steady state conditions.

2. Mathematical formulation

A TEC module (TECM) is composed of many thermoelectric pairs embedded inside it. By considering the periodicity of the thermal characteristics, only one pair is considered for the analysis, as shown in figure 1.

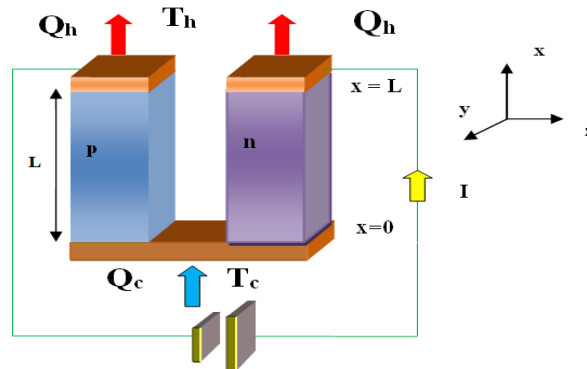


Figure 1. Simplified schema of a thermoelectric cooler.

As previously said, the working principle of these devices is the Peltier effect. When an applied current flows into the system, a cooling load Q_c is absorbed from the reservoir at T_c and an heating load Q_h is transferred to the reservoir at T_h . In order to perform the thermal behavior of the system, three additional effects have to be considered: the Fourier effect, the Joule effect and the Thomson effect. The following different assumptions underlie the development of the analytical model

- The material of the thermoelectric pair is homogeneous and isotropic so that the thermal conductivity and electric resistivity may be considered constant.
- Thermoelectric pellets are insulated thermally and electrically, except at the contact between the junctions and the two reservoirs which have fixed temperatures, T_h and T_c , respectively. The side surfaces of the TEC are considered adiabatic.
- The cross-sectional areas A_p and A_n and the lengths L_p and L_n of the thermoelements are respectively equal.
- Initially both semiconductors have a room temperature T_0 fixed at 298 K.
- The applied current is constant and uniform.

In this way, the transient thermal behaviour of both semiconductors (p and n-type) can be described by means of the 1-D heat flow governing equation along the x -direction, as shown in [4,5].

$$k_i \frac{\partial^2 T_i}{\partial x^2} \mp \gamma_i \frac{I}{A_i} \frac{\partial T_i}{\partial x} + \frac{I^2 R_i}{L_i A_i} = \rho c \frac{\partial T_i}{\partial t} \quad (2.1)$$

where the subscript i stands for n and p respectively. In detail, the plus sign is used for the n-type thermoelement, whereas the minus one is for the p-element. By using the dimensionless parameters introduced in [4,5] and here defined in appendix A, the temperature distributions may be obtained by solving the following dimensionless equations:

- Parabolic heat diffusion equations

$$\frac{\partial^2 \vartheta_n}{\partial \xi^2} + B_1 \frac{\partial \vartheta_n}{\partial \xi} + B_2 = \frac{\partial \vartheta_n}{\partial \tau} \quad (2.2)$$

$$\alpha_r \frac{\partial^2 \vartheta_p}{\partial \xi^2} - D_1 \frac{\partial \vartheta_p}{\partial \xi} + D_2 = \frac{\partial \vartheta_p}{\partial \tau} \quad (2.3)$$

- Boundary Conditions

$$\begin{aligned} \vartheta_n(\tau, 0) = \vartheta_p(\tau, 0) &= 1 \\ \vartheta_n(\tau, 1) = \vartheta_p(\tau, L_r) &= h \end{aligned} \quad (2.4)$$

- Initial Conditions

$$\vartheta_n(0, \xi) = \vartheta_p(0, \xi) = 0 \quad (2.5)$$

where the dimensionless coefficients B_i and D_i (with $i = 1$ or 2) are defined as follows.

$$B_1 = \frac{I \gamma_n L_n}{A_n k_n} \quad (2.6)$$

$$B_2 = \frac{I^2 L_n R_n}{A_n k_n (T_c - T_0)} \quad (2.7)$$

$$D_1 = \frac{I \gamma_p L_n}{A_p k_n C r} \quad (2.8)$$

$$D_2 = R_p I^2 L_n^2 [A_p k_n L_p (T_c - T_0) Cr]^{-1} \quad (2.9)$$

3. Solution of the governing equations

The temperature solutions have been carried out by using the well-established methods of Separation of Variables and the Laplace Transform as shown in the next subsections.

3.1. SOV method

Following the Ozisik's approach [11], the temperature solutions in both domains p and n are expressed as sum of a steady state part and a complementary transient part that is the solution of the associated transient homogeneous problem. We have:

$$\begin{aligned} \vartheta_n(\zeta, \tau) = & \frac{\exp(-B_1) - h - \frac{B_2}{B_1}}{\exp(-B_1) - 1} + \frac{h + \frac{B_2}{B_1} - 1}{\exp(-B_1) - 1} \exp(-B_1 \zeta) - \frac{B_2}{B_1} \zeta + \sum_{m_n=1}^{\infty} c_{m_n} \sin(\beta_{m_n} \zeta) \exp(-\beta_{m_n}^2 \tau) \\ & \times \exp\left(\frac{(-B_1)}{2} \zeta - \frac{(-B_1)^2}{4} \tau\right) \end{aligned} \quad (3.1)$$

$$\begin{aligned} \vartheta_p(\zeta, \tau) = & \frac{\exp\left(\frac{D_1}{\alpha_r} L_r\right) - h + \frac{D_2}{D_1} L_r}{\exp\left(\frac{D_1}{\alpha_r} L_r\right) - 1} + \frac{h - \frac{D_2}{D_1} L_r - 1}{\exp\left(\frac{D_1}{\alpha_r} L_r\right) - 1} \exp\left(\frac{D_1}{\alpha_r} \zeta\right) + \frac{D_2}{D_1} \zeta \\ & + \sum_{m_p=1}^{\infty} c_{m_p} \sin(\beta_{m_p} \zeta) \exp(-\alpha_r \beta_{m_p}^2 \tau) \exp\left(\frac{D_1}{2\alpha_r} \zeta - \frac{(D_1)^2}{4\alpha_r} \tau\right) \end{aligned} \quad (3.2)$$

Where and $\beta_{m_n} = m\pi$ $\beta_{m_p} = \frac{m\pi}{L_r}$ are the m eigenvalues of the problem and c_{m_n} and c_{m_p} are the integration constants depending on the initial conditions.

3.2. LT method

By applying Laplace transform to equations (2.2) and (2.3) as proposed in [4,5], we obtain

$$\Theta_n(s, \xi) = C_{1n}(s) \exp(l_{1n}(s)\xi) + C_{2n}(s) \exp(l_{2n}(s)\xi) + \frac{B_2}{s^2} \quad (3.3)$$

$$\Theta_p(s, \xi) = C_{1p}(s) \exp(l_{1p}(s)\xi) + C_{2p}(s) \exp(l_{2p}(s)\xi) + \frac{D_2}{s^2} \quad (3.4)$$

$$\Theta_n(s, 0) = \Theta_p(s, 0) = \frac{1}{s}$$

$$\Theta_n(s, 1) = \Theta_p(s, L_r) = \frac{h}{s} \quad (3.5)$$

$$\Theta_n(0, \zeta) = \Theta_p(0, \zeta) = 0$$

where $\Theta_j(s, \xi) = L[\vartheta(\xi, \tau)]$ with $j = n, p$. Two different approaches are used to solve the inverse Laplace Transform (ILT, for short), the analytical-based Riemann-sum approximation [4,5] and a numerical MATLAB[®] function [12]. By means of the former method obtain

$$\vartheta(\zeta, \tau) = \frac{\exp(\phi\tau)}{\tau} \left[\frac{1}{2} \Theta(\zeta, \phi) + \operatorname{Re} \sum_{n=1}^N \Theta \left(\zeta, \phi + \frac{i\pi n}{\tau} \right) (-1)^n \right] \quad (3.6)$$

where for a rapid convergence of the Riemann sum, ϕ has to be such that $\phi\tau \approx 4.7$ [4,5].

Note that i is the imaginary unit and Re denotes the real part of the complex summation.

3.3. Performance of the micro-TEC

Once the temperature distributions are known, the dimensionless cooling and the heating loads may be obtained as:

$$q_c = G - \frac{\partial \vartheta_n(\tau, 0)}{\partial \zeta} - k_r A_r \frac{\partial \vartheta_p(\tau, 0)}{\partial \zeta} \quad (3.7)$$

$$q_h = H - \frac{\partial \vartheta_n(\tau, 1)}{\partial \zeta} - k_r A_r \frac{\partial \vartheta_p(\tau, L_r)}{\partial \zeta} \quad (3.8)$$

where the coefficients G and H are the dimensionless contributions due to the Peltier effect. Therefore the COP (coefficient of performance) is given by:

$$COP = \frac{q_c}{q_h - q_c} \quad (3.9)$$

4. Results and discussion

A module consisting of 8 embedded thermoelectric pairs [10] has been considered for the simulations. The values of the semiconductor properties and their geometrical characteristics are listed in tables 1 and 2. The steady-state temperature profiles in presence and in absence of the Thomson effect are plotted in figures 2 where T_h is set at 300 K and T_c at 290 K with an electric current of 3.8A.

Table 1. Semiconductor elements properties and their geometrical sizes.

Parameter	p-type	n-type	Reference
k ($\text{Wm}^{-1}\text{K}^{-1}$)	1.472	1.643	[10]
A (m^2)	2.5×10^{-7}	2.5×10^{-7}	[10]
L (m)	5×10^{-4}	5×10^{-4}	[10]
ρ (kg m^{-3})	7740	7740	[9]
c ($\text{J kg}^{-1}\text{K}$)	187	187	[3]
r_e ($\Omega \text{ m}$)	8.826×10^{-6}	8.239×10^{-6}	[10]

Table 2. Seebeck coefficients [10], [13].

	p-type $(\text{Bi}_{0.25}\text{Sb}_{0.75})_2\text{Te}_3$	n-type $\text{Bi}_2(\text{Te}_{0.94}\text{Se}_{0.06})_3$
σ (VK ⁻¹)	-6.95×10^{-10} $(T-300)^2 + 3.42 \times 10^{-7}$ $(T-300) + 2.207 \times 10^{-4}$	1.04×10^{-9} $(T-300)^2 - 1.25 \times 10^{-7}$ $(T-300) - 2.23 \times 10^{-4}$

The steady state temperature profiles for both semiconductors are slightly lower than the results obtained numerically in [10], with a maximum temperature difference of 6.6 K between the two pellets compared with the 7-8 K obtained in [10]. This is due to the different solution method and to the different evaluation of the Seebeck and Thomson coefficients.

With reference to the steady state cooling loads in presence and in absence of the Thomson effect (figure 3), the maximum value of Q_c is 1.926 W with Thomson effect and 1.774 W without Thomson effect.

As regards the steady state COP (figure 4), a slightly higher difference with the results in [10] may be underlined. In fact the COP values with and without Thomson effect shown in [10] seem to be coincident (4.84 at 0.292 A), whereas, in the present paper the maximum value for the steady state COP in presence of Thomson effect is 4.84 at 0.3 A and nearly 4.4 in absence of Thomson effect.

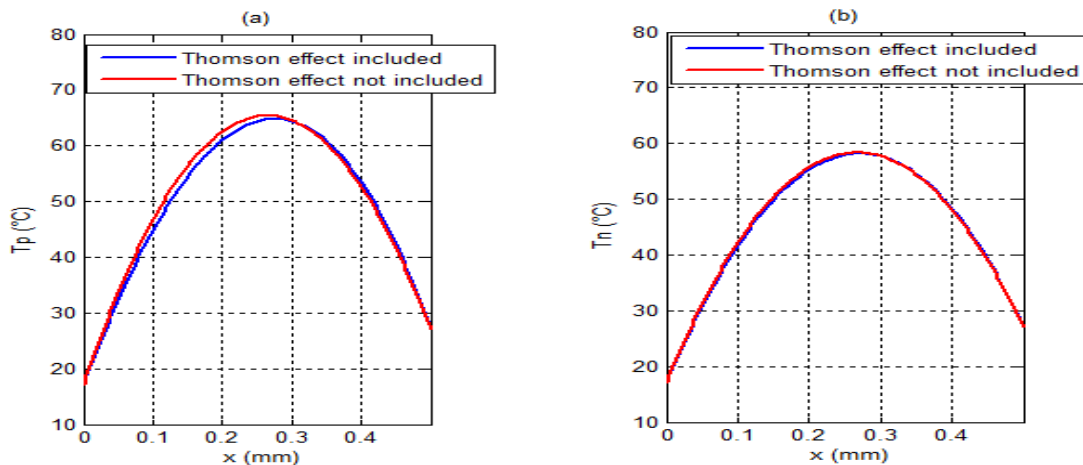


Figure 2. Steady-state T profiles in the semiconductors a) p-type and b) n-type.

The transient temperature profiles are shown in figure 5, (a) and (b), including the Thomson effect with an electric current of 3.8 A. Note that the temperature profiles for times $t < 2$ ms are plotted only by using the SOV and the numerical ILT methods, as the analytical ILT does not converge for dimensionless times shorter than 0.01 (to which corresponds a dimensional of 2ms). During the simulations we have taken $N=2000$ in the Riemann sum, defined in equation (3.6). For dimensionless times higher than 0.01 no difference between the three techniques arises.

A more accurate analysis is required for the transient performances of the device, i.e. the cooling load Q_c and the COP, shown in figures 6 and 7, respectively. As regards Q_c , the different values obtained are listed in table 3. It can be seen that at very early times, less than 2 ms, the AILT does not yield physically- consistent results, whereas the other two techniques may also be used only for time values less than 2 ms, but greater than 0.1 ms. This is due to the imposed non-realistic time-independent boundary conditions of the first kind. For time values higher than 2 ms the three techniques give the same results. The maximum Q_c value is of 2.89 W and occurs at 3.4 ms.

Different COP profiles are shown in figure 7. The maximum COP value of about 2 obtained with the different techniques occurs after 1.66 ms and was obtained by using the SOV and the NILT methods, as the AILT (based on the Riemann sum Approximation) is numerically unstable at early times

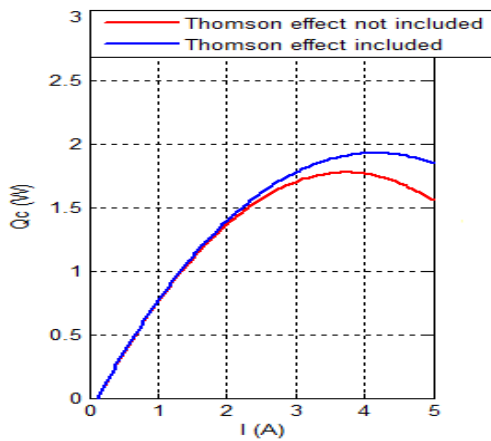


Figure 3. Steady state cooling load.

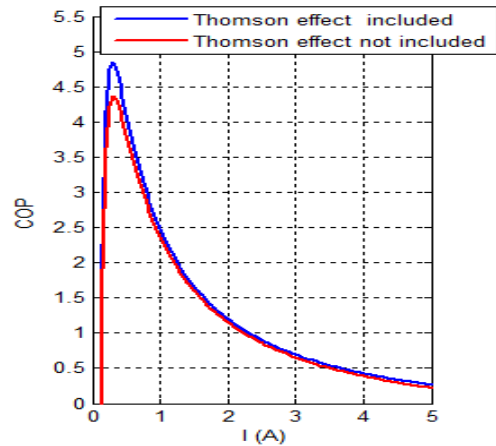


Figure 4. Steady state COP.

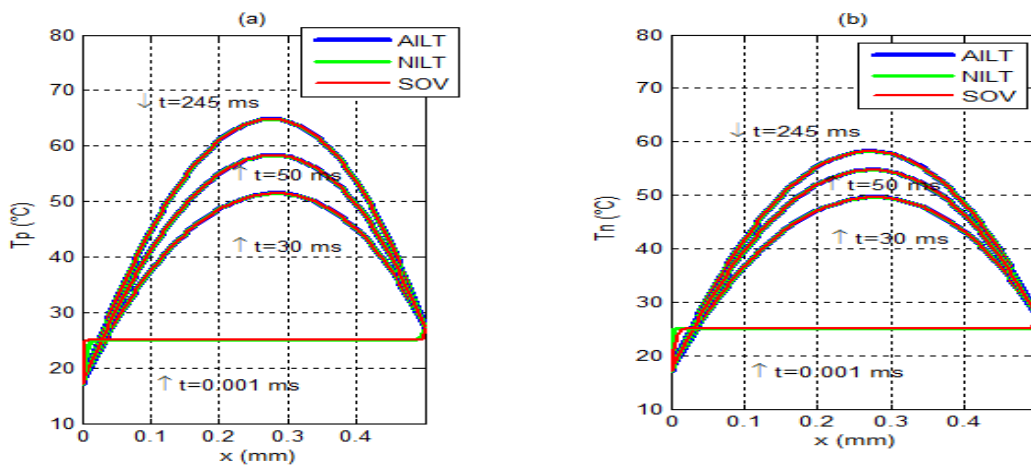


Figure 5. Transient T profiles in the semiconductors a) p-type and (b) n-type. AILT stands for analytical inverse Laplace Transform, NILT stands for numerical inverse Laplace Transform.

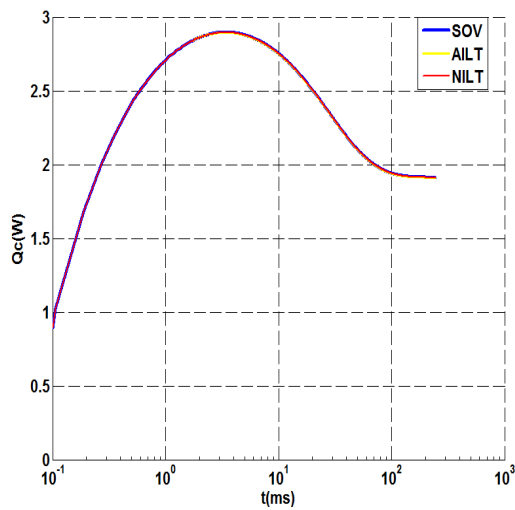


Figure 6. Transient Q_c profiles with the three techniques.

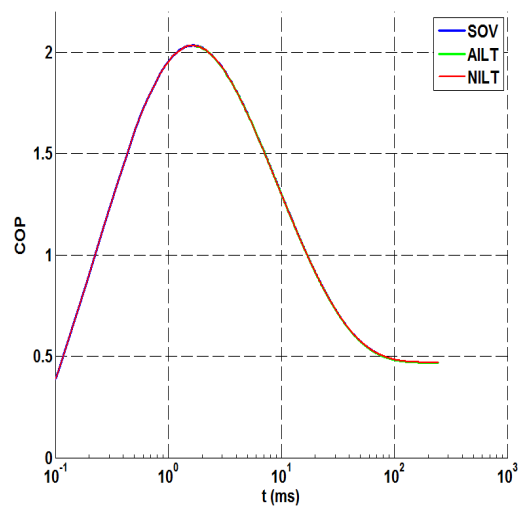


Figure 7. Transient COP profiles with the three techniques.

Table 3. Comparison among the Q_c values obtained with the different techniques.

t (ms)	Q_{c_SOV} (W)	Q_{c_NILT} (W)	Q_{c_AILT} (W)	COP_SOV	COP_NILT	COP_AILT
0.100	0.911	0.912	-	0.365	0.365	-
0.200	1.722	1.722	-	0.891	0.891	-
1.000	2.710	2.710	-	1.955	1.954	-
2.000	2.860	2.860	2.860	2.021	2.020	2.020
3.000	2.893	2.893	2.893	1.928	1.928	1.928
4.000	2.892	2.892	2.892	1.805	1.803	1.803
5.000	2.877	2.877	2.877	1.697	1.696	1.696
10.000	2.715	2.715	2.715	1.302	1.300	1.300
15.000	2.626	2.626	2.626	1.070	1.069	1.069
20.000	2.510	2.510	2.510	0.918	0.916	0.916
30.000	2.324	2.323	2.323	0.735	0.734	0.734
50.000	2.106	2.105	2.105	0.577	0.576	0.577
100.000	1.941	1.941	1.941	0.484	0.483	0.483

The investigation of the hyperbolic heat diffusion equation by using Green's functions [14] for a more realistic description of the micro-TEC transient behaviour at early times remains a subject of the future research.

5. Conclusion

Three different approaches for the thermal transient modelling of a micro-thermoelectric cooler have been presented and compared. The Inverse Laplace Transform performed analytically by Riemann sum approximation does not allow its transient thermal behaviour to be modelled for very short times (less than 1.719 ms). As regard the cooling load and COP, the SOV and NILT cannot be used for times less than 0.1 ms, due to the simplifying assumption of time-independent boundary

conditions. An important remark is for the COP and Q_c that, during the transient behaviour, reach a maximum value at different times.

A comparison of the results with data available in the literature (and obtained both experimentally and numerically - by FEM) indicates the good accuracy of the proposed solution methods under steady state conditions.

Appendix A. Nomenclature

A = cross-sectional area

A_r = cross-sectional area ratio = A_p/A_n

c = specific heat

Cr = dimensionless heat capacity = $\rho_p c_p / \rho_n c_n$

h = temperature ratio = $(T_h - T_0) / (T_c - T_0)$

I = electric current

J = current density

k = thermal conductivity

k_r = thermal conductivity ratio = k_p/k_n

L = length

$L_r = L_p/L_n$ = Length ratio

Q_c = Cooling load

Q_h = Heating load

q_c = Dimensionless cooling load = $Q_c L_n / (k_n A_n (T_c - T_0))$

q_h = Dimensionless heating load = $Q_h L_n / (k_n A_n (T_c - T_0))$

R = electric resistance

r_e = electric resistivity

t = time

T = temperature

T_0 = room temperature

x = space coordinate

Greek symbols

α = thermal diffusivity

$\alpha_r = \alpha_p / \alpha_n$ = dimensionless thermal diffusivity

γ = Thomson coefficient, defined as $\gamma = T d\sigma / dT$

ϑ = dimensionless $T = (T - T_0) / (T_c - T_0)$

ξ = dimensionless space = x/L

ρ = density

σ = Seebeck coefficient.

τ = dimensionless time = $\alpha t L^{-2}$

Subscripts

c = cold

h = hot

n = semiconductor n

p = semiconductor p

References

- [1] Yang R, Chen G, Kumar A R, Snyder G J and Fleurial J P 2005 Transient cooling of thermoelectric coolers and its applications for microdevices *Energy Conv. Manag.* **46** 1407-21
- [2] Zhao D and Tan G 2014 A review of thermoelectric cooling: Materials, modeling and applications *Appl. Therm. Eng.* **66** 15-24
- [3] Cheng C H, Huang S Y and Cheng T C 2010 A three-dimensional theoretical model for predicting transient thermal behaviour of thermoelectric coolers *Int. J. Heat and Mass Transfer* **53** 2001-11
- [4] Naji M, Alata M A and Al Nimr M 2003 Transient behaviour of a thermoelectric device *Proc. Inst. Mechan.Eng. A J. Power Energy* **17** 615-621
- [5] Naji M, Alata M A and Al Nimr M 2003 Transient behaviour of a thermoelectric device under the hyperbolic heat conduction model *Int. J. Thermophys.* **24** 1753-68
- [6] Wang X D, Huang Y X, Cheng C H, Lin D T W and Kang C H 2012 A three dimensional numerical modeling of thermoelectric device with consideration of coupling of temperature field and electric potential field *Energy* **47** 488-497
- [7] Meng J H, Wang X D and Zhang X X, 2013 Transient modeling and dynamic characteristics of thermoelectric cooler *Appl. Energy* **108** 340-348
- [8] Cheng C H and Huang S Y 2012 Development of a non-uniform-current model for predicting transient thermal behavior of thermoelectric coolers *Appl. Energy* **100** 326-335
- [9] Zhu W, Deng Y, Wang Y and Wang A 2013 Finite element analysis of miniature thermoelectric coolers with high cooling performance and short response time *Microelectron. J.* **44** 860-868
- [10] Chen W H, Liao C Y and Hung C I 2012 A numerical study on the performance of miniature thermoelectric cooler affected by Thomson effect *Appl. Energy* **89** 464-473
- [11] Özisik M N 1993 *Heat Conduction* (New York: Wiley)
- [12] Hollenbeck K J 1998 INVLAP.M: A matlab function for numerical inversion of Laplace transforms by the de Hoog algorithm <http://www.isva.dtu.dk/staff/karl/invlap.htm>
- [13] Yamashita O 2009 Effect of linear and non-linear components in the temperature dependences of thermoelectric properties on the cooling performance *Appl. Energy* **86** 1746-56
- [14] Haji-Sheikh A, de Monte F and Beck J V 2013 Temperature solution in thin films using thermal wave Green's function solution equation *Int. J. Heat and Mass Transfer* **62** 78-86